Glimpses into the petrogenesis of some classical lithotypes from the Fen carbonatite complexes, Norway

A Thesis submitted to

Indian Institute of Science Education and Research Pune

in partial fulfillment of the requirements for the

BS-MS Dual Degree Programme

By

Varaprasad Tonta

Indian Institute of Science Education and Research Pune

Dr. Homi Bhabha Road, Pashan, Pune 411008,

INDIA.

March, 2024

Supervisor: Raymond A. Duraiswamy

This Thesis is dedicated to my parents

Certificate

This is to certify that this dissertation entitled "**Glimpses into the petrogenesis of some classical lithotypes from the Fen carbonatite complexes, Norway**" towards the partial fulfillment of the BS-MS dual degree programme at the Indian Institute of Science Education and Research, Pune represents study/work carried out by Varaprasad Tonta Indian Institute of Science Education and Research under the supervision of Raymond A. Duraiswami, Assistant Professor Department of Geology, Savitribai Phule Pune University, during the academic year 2023-2024.

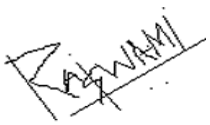

Raymond A. Duraiswami

Date: 27-03-2024

Committee:

Supervisor: Dr. Raymond A. Duraiswami, SPPU Pune

Expert Member: Dr. Sudipta Sarkar, IISER PUNE.

Declaration

I hereby declare that the matter embodied in the report entitled "**Glimpses into the petrogenesis of some classical lithotypes from the Fen carbonatite complexes, Norway**" are the results of the work carried out by me at the Department of Geology, Indian Institute of Science Education and Research, Pune, and Savitribai Phule Pune University under the supervision of Raymond A. Duraiswami and the same has not been submitted elsewhere for any other degree.

Varaprasad Tonta

Date: 27-03-2024

Acknowledgments

I would like to express my sincere gratitude to Prof. Raymond A. Duraiswami for his exceptional guidance and support as my supervisor during my Master's project. His expertise and mentorship have been invaluable to my research and academic development.

I am also thankful to Prof. Sudipta Sarkar and Prof. Gyana Ranjan Tripathi from IISER Pune for allowing me to use the instruments at IISER, which were essential for completing my project. Special thanks to Prof. Srinivas Hotha for helping me obtain permission to use the XRD facilities.

I am deeply grateful to my parents for their love, support, and encouragement throughout this journey. Their sacrifices and guidance have been crucial to my success. I also thank my sisters, Vanaja and Vani, for their unwavering belief in me and constant support.

I would like to acknowledge IISER Pune and SPPU for providing the resources and support needed for my research, particularly access to the XRD and XRF facilities.

My sincere thanks go to Dr. Sudha Rajamani for the financial support and assistance with food subsidies, which were essential for me to pursue my studies.

I am thankful to my lab mates, Mr. Parag, Miss Apoorva, and Mr. Hemanth, for their support and encouragement throughout my research.

Lastly, I am grateful to all my friends, volleyball group and seniors (Peddi Raju, Balakrishna, Sanjay Golla) for their companionship and support over the years.

Table of Contents

List of Figures

Abstract

Carbonatites, rare igneous rocks rich in carbonate minerals, hold significant economic value due to their high concentrations of niobium, tantalum, and rare earth elements (REEs). Despite their importance, the origins and evolution of carbonatites remain subjects of ongoing scientific debate. In this study, I investigate the genesis of the Fen Carbonatite Complex in Norway through a comprehensive analysis of its mineralogy and geochemistry. Employing petrography, X-ray diffraction (XRD), X-ray fluorescence (XRF), and inductively coupled plasma mass spectrometry (ICP-MS), I've explored two primary hypotheses for the origin of carbonatites: magmatic crystallization and hydrothermal metasomatism.

My findings reveal a multifaceted petrogenesis for the Fen Carbonatite Complex, with evidence supporting both magmatic and hydrothermal processes. The magmatic origin is indicated by significant REE enrichments, particularly heavy rare earth elements (HREEs), and the presence of primary magmatic minerals such as calcite, dolomite, and apatite. However, the exceptional enrichments in middle and light rare earth elements (MREEs and LREEs) point to substantial metasomatic modification, likely driven by external fluid interactions.

Textural features observed through petrographic analysis, such as ghost crystals and pseudo cubic fluorite, alongside geochemical trends from major oxide analysis, further corroborate the role of metasomatic processes. The interplay of magmatic and metasomatic influences underscores the complex evolution of the Fen Carbonatite Complex.

I conclude that while the Fen Carbonatite Complex exhibits strong magmatic characteristics, its development has been significantly shaped by hydrothermal and metasomatic processes. The integration of multiple analytical techniques has been essential in unraveling the intricate formation history of these rocks. This research highlights the necessity of considering both magmatic and metasomatic theories to fully understand the petrogenesis of carbonatites, contributing valuable insights to the broader geological understanding of these economically important rocks.

1. Introduction

1.1 Background

1.1.1 What are Carbonatites?

Carbonatites are a unique and relatively rare type of igneous, intrusive, and extrusive rocks containing more than 50% carbonate minerals by volume(Streckeisen, 1979). Despite their scarcity, carbonatites hold significant importance due to their unique geochemical signatures and economic mineral deposits. Carbonatites are notable for their distinct geochemical signatures, characterized by high concentrations of incompatible elements such as niobium, tantalum, and rare earth elements (REEs). These economically significant elements often occur in carbonatite deposits, making them valuable targets for mineral exploration and extraction.

The study of carbonatites is essential for understanding the dynamics of the Earth's mantle and identifying potential sources of critical raw materials necessary for modern technologies. Research into carbonatites encompasses various disciplines, including petrology, geochemistry, mineralogy, and economic geology, contributing to our broader understanding of Earth's geological processes and the formation of mineral resources

1.1.2 Origin of Carbonatites

The genesis or the mechanisms of carbonatites formation have been a subject of debate, with several hypotheses proposed to explain their genesis. My work aims to identify the critical minerology that host the rare earth minerals and unravel the mystery of carbonatites, which presents us with two intriguing hypotheses: a magmatic origin and/or a hydrothermal origin. The magmatic origin hypothesis proposes that carbonatites form directly from primary melts from the upper mantle enriched in carbonate components, either through partial melting or immiscibility processes within the magma chamber.(Yaxley et al., 2022) This theory suggests that carbonatitic melts rise to the Earth's surface and crystallize, forming carbonatite complexes that are

closely associated with nepheline syenites. Conversely, the hydrothermal origin hypothesis suggests that carbonatites result from metasomatic processes involving the infiltration of carbonate-rich fluids into pre-existing carbonatite rocks, by replacement of silicate minerals with carbonate minerals. These hydrothermal fluids may originate from deep-seated sources, such as the mantle, or from shallower crustal reservoirs.

1.2 Study area

The Fen Complex, Norway (Fig. 1) is one of the classical carbonatite complexes of the World (Brogger 1921). The complex was subsequently studied by several workers (Sæther, 1957; (Ramberg, 1973) Griffin and Taylor, 1975; (Mitchell & Brunfelt, n.d.) who reconfirmed and advanced the petrological inference that carbonatites were indeed of igneous origin. The Fen complex has an exposed area of ~6 km^2 and mainly consists of carbonatite-ijolite-pyroxenite complex (Bergstøl and Svinndal, 1960).

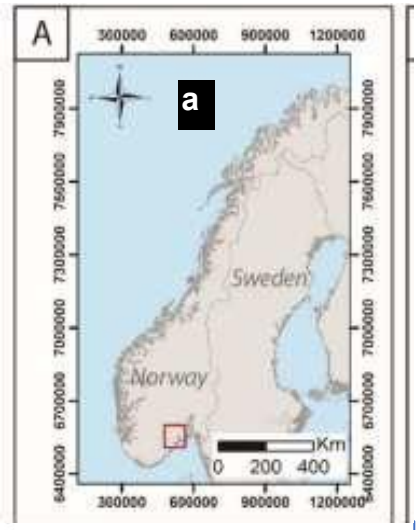

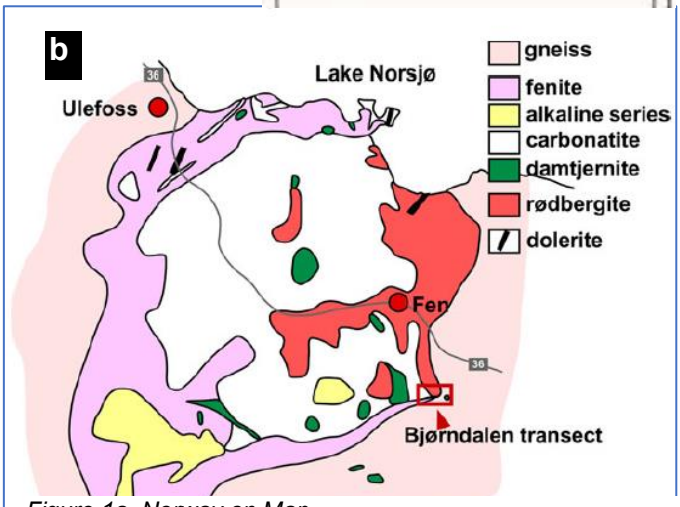

Figure 1a. Norway on Map

1b. Simplified geological map of the Fen Complex, Norway (Saether, 1957)

The complex is intruded by several ultramafic lamprophyres (Damtjernite), the phogophite from which was dated at 583 ± 15 Ma by the $^{40}Ar/^{39}Ar$ method (Meert et al., 1998).The carbonatites at Fen complex can be classified into sovite, beforsite (dolomite carbonatite) and altered, hematite-richcarbonatite known as rødbergite.A review of previous literature reveals the following major and accessory minerals associated with different rock types at Fen Complex, Norway: The hydrothermally altered rødbergites locally contain high grades (up to 1.6 wt.%) total REE ((Andersen, 1984), (Andersen, 1988) ; (Marien et al., 2018a)).

Rock type	Sub-rock type	Major minerals	Accessory mineral
Carbonatite	Sovite/ rauhaugite	Calcite, dolomite, apatite, pyrite, columbite	Quartz, barite, pyrochlore, fluorite, REE flurocarbonate (Ce-synchysite and parisite)
	Transitional Rodbergite	Calcite, dolomite,	Barite, Ba bearing biotite, apatite, Ce-monazite,quartz, hematite
	Rodbergite	Fe-dolomite, barite, Ba bearing biotite, hematite	Calcite, apatite, quartz, Ce-monazite, allanite, fluorite
Fenite	Sodic fenite	Quartz, feldspare, chlorite, opaques	Ankerite

1.3 Objectives of the study

Using Petrography, XRD, XRF, ICP-MS techniques, I aim to find the mineralogy and unravel the complex origin and evolution of carbonatites by exploring the contrasting mechanisms of magmatic and hydrothermal origins, this thesis aims to elucidate the dominant processes driving the formation of FEN Carbonatite complex situated in Norway.

2. Methodology

The following methodology adopted during this study:

1. **Literature review:** Literature survey on the Fen carbonatite and allied aspects was undertaken by me. Published papers were collected by my supervisor from various University libraries, Carbonatite Research Center, Ambadongar, Indian Institute of Technology (Powai), Mumbai, etc. and these were made available to me. I also obtained relevant literature from the Internet.

2. **Geological sampling:** The samples collected by my Supervisor Dr. RA Duraiswami and his student miss. Apoorva Chordiya have been used in this study.

Figure 2 Fen51-56 Geological Monument, Miss. Apoorva Chordiya in the picture

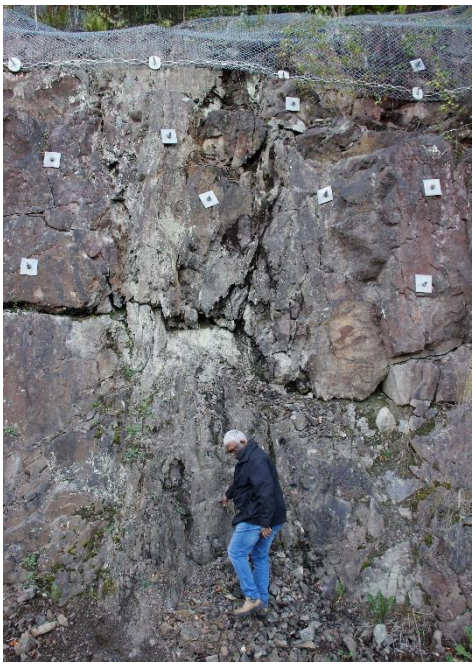

Figure 2 Fen65-2-67-2 Rodbergite section

Figure 4

a) Sovite,

b) Sovite 1,

c) Finite

3. **Laboratory work:** I undertook detailed petrographic and textural studies. XRD of powders was also undertaken by me. I also subjected the powered samples to detailed geochemical analysis i.e. major oxide (XRF), trace and REE (ICPMS).
4. **Synthesis of the data, report writing and submission:** The data generated during the laboratory was synthesized, interpreted and is produced in this thesis.

In this chapter, I will first provide an overview and methodologies of the employed analytical techniques—Petrography, Powder X-ray Diffraction (XRD), X-ray Fluorescence (XRF), and Inductively Coupled Plasma Mass Spectrometry (ICP-MS) this introduction will provide readers with a fundamental understanding of these techniques and why do I used these techniques.

2.1 Analytical Techniques

2.1.1 Overview of Petrography, XRD, XRF, ICP-MS

Petrographic analysis offers insights into the mineralogy, texture, and structural features of carbonatites, aiding in the interpretation of their petrogenesis and alteration processes.

Where minerals cannot be identified due to fine grain size powder X-ray diffraction (XRD) emerges as a robust tool, facilitating the identification of major minerals within carbonatite samples, thus enabling comprehensive mineralogical characterization. I am employing two complementary approaches to delve deeper into the magmatic origin theory. First, meticulously analyzing major oxide elements to gain valuable insights into the composition of the Fen carbonatite complex. Simultaneously, utilizing advanced X-ray diffraction (XRD) techniques to explore the magmatic components within the Fen carbonatite complex. Inductively Coupled Plasma Mass Spectrometry (ICP-MS) detects trace elements at low concentrations, providing accurate quantification. Simultaneously analyzes multiple elements and isotopes, offering comprehensive data. ICP-MS is widely used in environmental and geological research, contributing to our understanding of Earth's processes.

By integrating these analytical techniques, this thesis aims to elucidate the genesis of

carbonatites, focusing on two hypotheses: magmatic and hydrothermal origins. Case studies from the Fen Complex in Norway and Kangankunde in South Africa provide valuable insights into the formation mechanisms of carbonatites and shed light on their geological significance.

2.1.2 X Ray Diffraction Methodology

The Powder XRD provides a powerful tool for identifying major minerals present in carbonatite samples, facilitating mineralogical characterization without requiring crystalline phase identification. samples were finely ground into a powder using a Agate Mortar and pestle. Once the samples are finely powdered, sample is placed on the glass slide (cleaned with ethanol and distilled water) and pressed with another slide and removed excess powder then loaded the sample. Using a copper Ka X-ray source (wavelength: 0.15406 nm) at 40kV and 30 mA filament emission, I've scanned samples over a 2-theta range of 5° to 59.99°. Scattered X-ray intensity was measured at 0.55-second intervals per step, with a step size of 0.019608. Utilized a rotation system to ensure thorough sample coverage. XRD analysis was conducted on 31 samples, identifying minerals by matching unknown peaks with standard peaks based on 2-theta angles and D spacing, which I have given in the results section. This process involves search and match procedures, utilizing a vast database of material standards. Manual searching is a well-established method, commonly used for mineral identification, offering distinct advantages.

Figure 3 Bruker's Powder X-Ray Diffractometer

(IISER Pune Physics department)

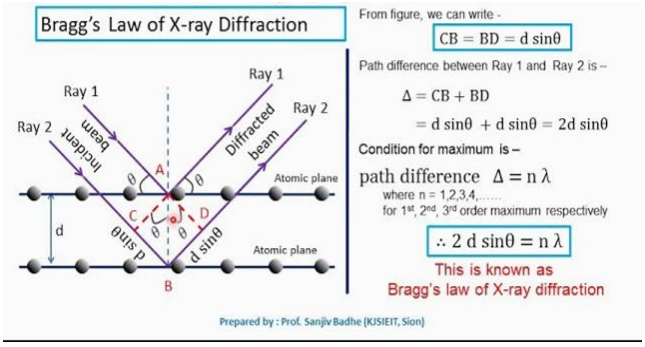

2.1.3 X Ray Fluorescence

XRF enables rapid and accurate determination of the elemental composition of carbonatites, including major, minor, and trace elements, contributing to a comprehensive understanding of their geochemical signatures and elemental abundances. XRF is done for 18 samples in two different batches.

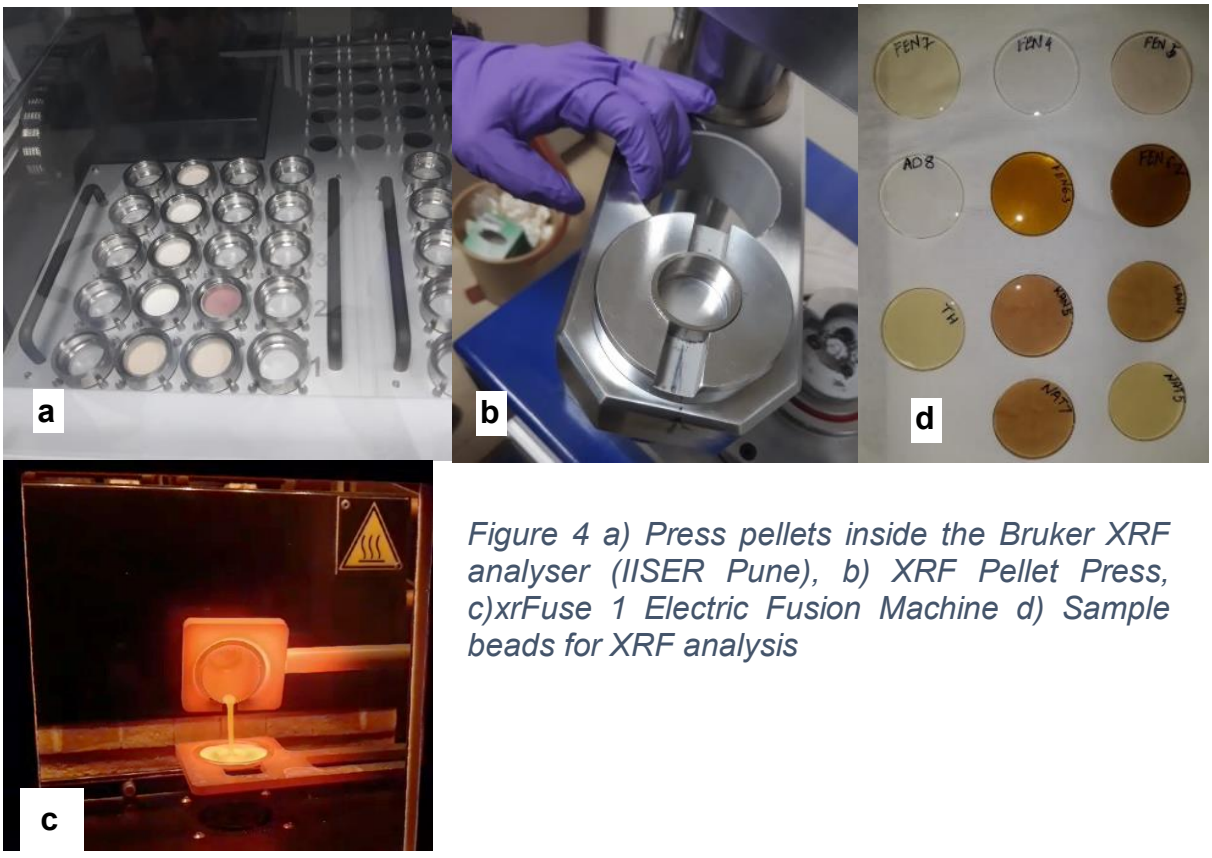

Figure 4 a) Press pellets inside the Bruker XRF analyser (IISER Pune), b) XRF Pellet Press, c)xrFuse 1 Electric Fusion Machine d) Sample beads for XRF analysis

For first batch 11 samples 0.55g of sample added to 9.35g of flux (Lithium tetraborate 66%) and mixed properly then 5 to 6 drops of 25% of LiBr solution is added and placed into the XRF heat fusion in which it had gone through different stages like, over 1100oC for 4 min melt time, 6 min shake time, 7:45 min of cooling time after these stages sample breads are removed carefully and placed as shown in the figure. Later cleaned the sample holders and gave sonorous treatment and after it dried and ready followed the same procedure for the remaining samples. For second batch of samples, 2.00 g of binder(cellulose) is measured and 8.00g of sample is added and using press prepared pellets (See fig). Then placed the sample pellets into Bruker WD X-ray Fluorescence (XRF) and done XRF. This study presents a comprehensive analytical approach integrating Bruker WD X-ray Fluorescence (XRF) spectroscopy with the

CIPW (Cation-Anion Proportional Weight) norm calculation method for the characterization of carbonatite samples. The XRF analysis was conducted using a Bruker XRF analyzer equipped with a rhodium (Rh) X-ray tube, operating at 50 kV and 40 mA. Calibration of the XRF spectrometer was meticulously performed using certified reference materials to ensure accurate and precise elemental quantification. The Bruker XRF analyzer measures the major oxide concentrations using the Geoquant Advance standard calibration method, providing an accuracy and precision of ±2% and ±1%. Elemental concentrations obtained from XRF analysis were then converted to oxide concentrations, essential for subsequent CIPW norm calculations.

The CIPW norm calculation method is a fundamental approach in petrology for estimating the mineralogical composition of rocks based on bulk chemical analysis. Unlike analytical techniques such as XRF, which directly measure elemental concentrations, the CIPW method utilizes chemical data obtained from analytical techniques like XRF, X-ray Diffraction (XRD), or chemical analysis. In the CIPW method, the chemical compositions of rocks are converted into proportions of idealized minerals, representing a theoretical mineral assemblage that could potentially exist in the rock. This conversion involves assigning cations and anions to different mineral species based on their chemical affinities and stoichiometries. By balancing cations and anions within the rock sample, the CIPW method ensures charge neutrality while respecting the chemical constraints imposed by mineral structures.

The normative mineral compositions were calculated using SINCLAS program of ((Verma et al., 2002). The program calculates the anhydrous recalculated data, gives a rock name following the Total Alkali Silica (TAS) diagram and also fixes the Fe2O3: FeO ratio for the given rock name and then calculates the norm. The SINCLAS program proved very useful as it provided the option of taking into account the subdivision of total iron. In the measured iron-oxidation ratio option, all iron was considered as Fe2O3(T) the Middlemost option (Middlemost, 1989) was used, which proposed a fixed ratio of Fe2O3 to FeO that depended on the rock type (classification). Following this recommendation, the SINCLAS program adjusts the Fe2O3: FeO ratio according to the rock type, readjusts the complete chemical data and classifies the sample. The major oxide and normative mineralogy obtained were used to classify the rock.

Using the calculated oxide concentrations, CIPW norms were determined, representing the proportions of idealized mineral phases in the carbonatite samples. These calculated norms were then compared with established mineral assemblages to identify the most likely mineral constituents present in the samples. The integration of XRF analysis with the CIPW norm calculation method provides a robust framework for the comprehensive characterization of carbonatites, offering valuable insights into their geochemical and petrological characteristics, petrogenesis, origin, and geological history.

One must not forget that when a sample is heated to high temperatures in the XRF instrument, volatile compounds such as water, carbon dioxide, and other organic materials are released as gases. The loss in weight of the sample due to the volatilization of these components is quantified as the LOI.

In the context of my work on carbonatites, LOI is particularly important because carbonatites often contain significant amounts of carbonate minerals, which can release carbon dioxide when heated. By measuring the LOI, we accurately account for the loss of carbon dioxide during the XRF analysis. This ensures that the final elemental concentrations obtained from XRF analysis are corrected for the loss of volatile components, providing more accurate and reliable results.

2.1.4 Petrography

Petrographic analysis offers insights into the mineralogy, texture, and structural features of carbonatites, aiding in the interpretation of their petrogenesis and alteration processes. While identification of minerals is crucial for correlation of minerals

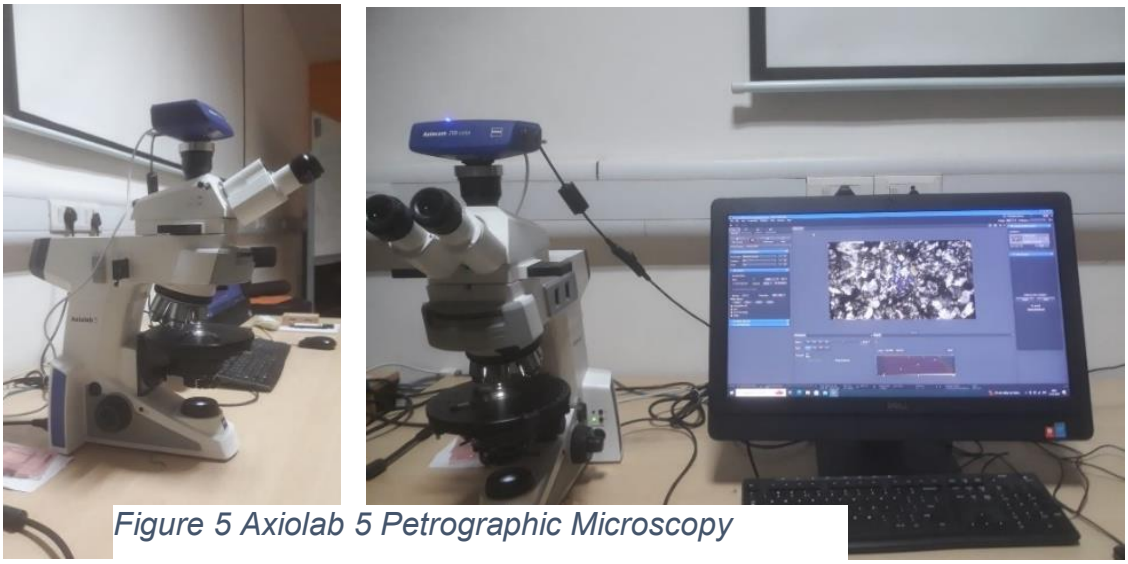

Figure 5 Axiolab 5 Petrographic Microscopy

occurrences with XRD of powders, they are very important for correlation with the overall geochemistry from XRF and ICPMS. The textures provide evidences for cooling in story and/or hydrothermal or metasomatic activity.

2.1.5 ICP – MS

ICP-MS, with its high sensitivity and precision, allows for the simultaneous analysis of trace elements and isotopes in carbonatite samples, providing crucial information on elemental distributions, isotopic signatures, and geochemical processes.

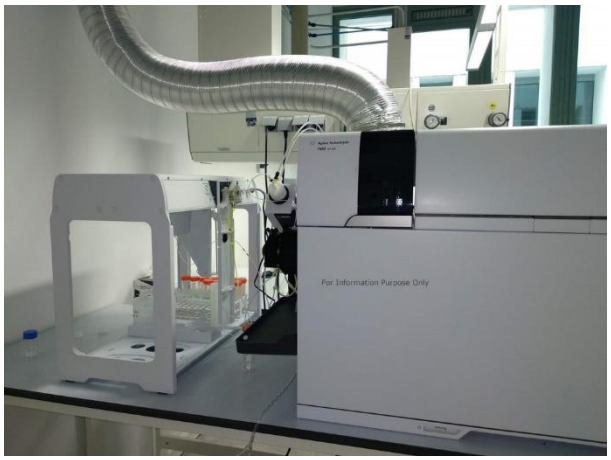

Figure 6 AGILENT 7800 ICP-MS LA

0.100g of sample measured and transferred into a Volumetric flask, then prepared Aqua regia by adding 20 ml HNO3 added to 60 ml of HCl (1:3 ratio of HNO3: HCl) is used to digest solid samples. then added this mixture of concentrated acids to the sample.

After that using hot plate, I've heated (at 120-200°C) the digestion vessel containing the acid and sample for 6 to 7 hours constantly monitoring. Next day I added some Distilled water to few samples and 2% HNO3 to few samples and continued heating. 2 FEN samples (FEN 5,7) still contained some undigested sample so I transferred those sample solutions to Teflon vessels and added 2-3 drops of HF to digest it properly and then added boric acid to neutralize the samples. I've heated for one more day, evaporated to dryness. Dried sample dissolved in Millipore water plus HNO_3 for acidification and then after we see transparent solutions with nothing left undigested, I've allowed the digestion vessel to cool to room temperature. Later allowed the digestion vessel to cool to room temperature. afterwards made it to volume of 100 ml by adding Distilled water.

3. Results and Discussion

3.1 Petrography

Fenitised gneiss

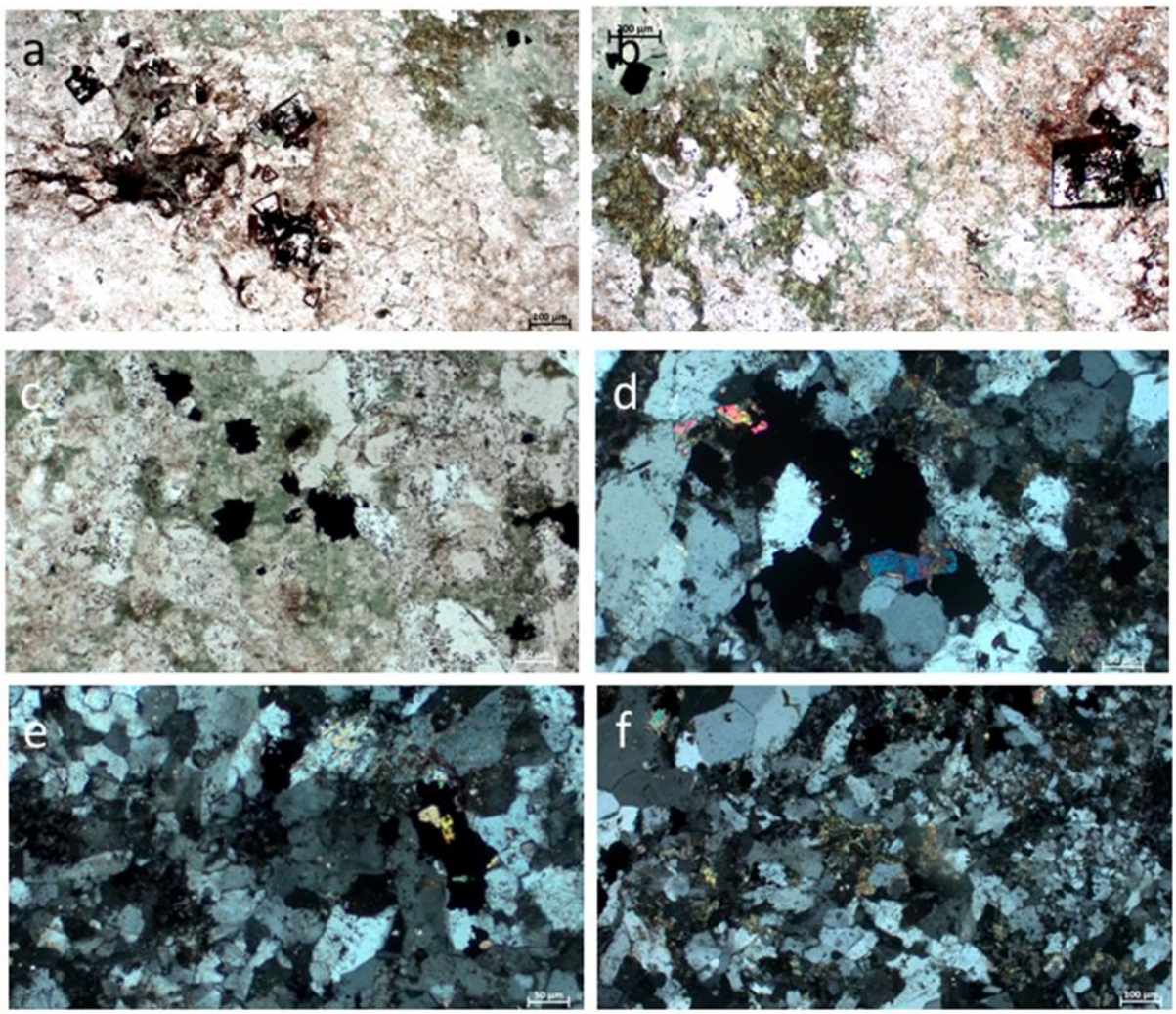

Figure 7 : Photomicrographs from fenitised gneiss (sample FEN 66_2). (a) Ghost crystals or pseudo ankerite crystals in a quartzo-feldspathic matrix. (b) Close up of a larger pseudocubic flourite crystals. Note the greenish brown chlorite-pyroxene-opaque association in the quartzo-feldspathic groundmass. (c) Accumulation of ahedral grains of opaques (magnetite?) in felsic matrix. (d) Another view of the opaque-biotite-quartzo-feldspathic matrix. (e) Biotite-magnetite (?) association in quartzo-feldspathic matrix. (f) fine-grained gnessic matrix away from the fenirised zone. Photomicrographs d, e, f between cross nichols, all other photos in plane polarised light

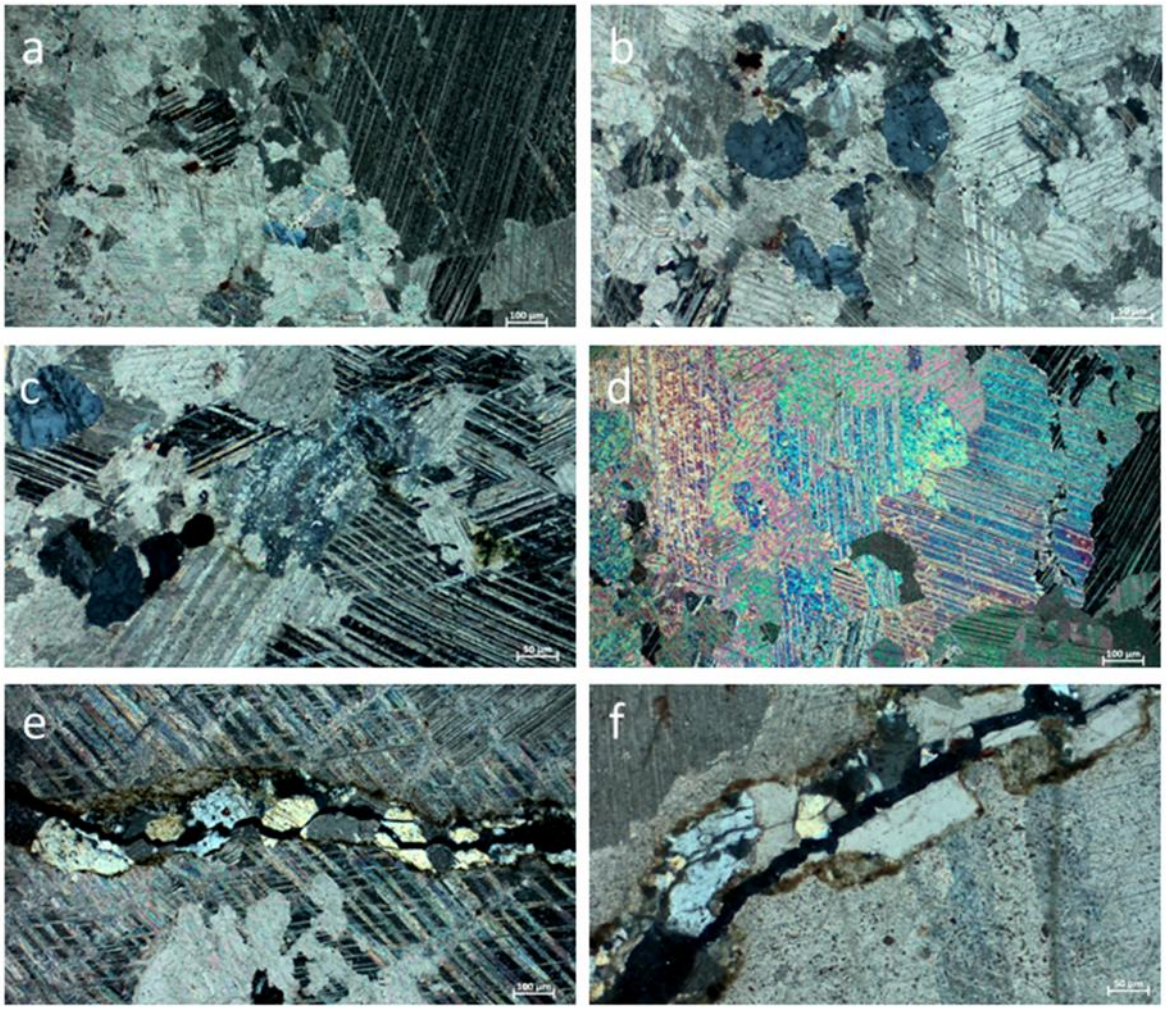

Figure 8 : Photomicrographs of sample sovite carbonatite (FEN 52). (a) Large calcite phenocryst surrounded by smaller sized calcite crystals. (b) small felsic (feldspar?) globules in the calcite groundmass. (c) irregular feldspar crystals within a predominantly calcite matrix. (d) Highly birefrengent (strontium rich?) calcite showing interlocking grain boundaries. (e) Sinuous vein cutting across the calcite fabric. (f) Close up of the vein showing calcite and feldspar. Note the alteration front in the calcite adjacent to the vein. All photomicrographs between cross nichols.

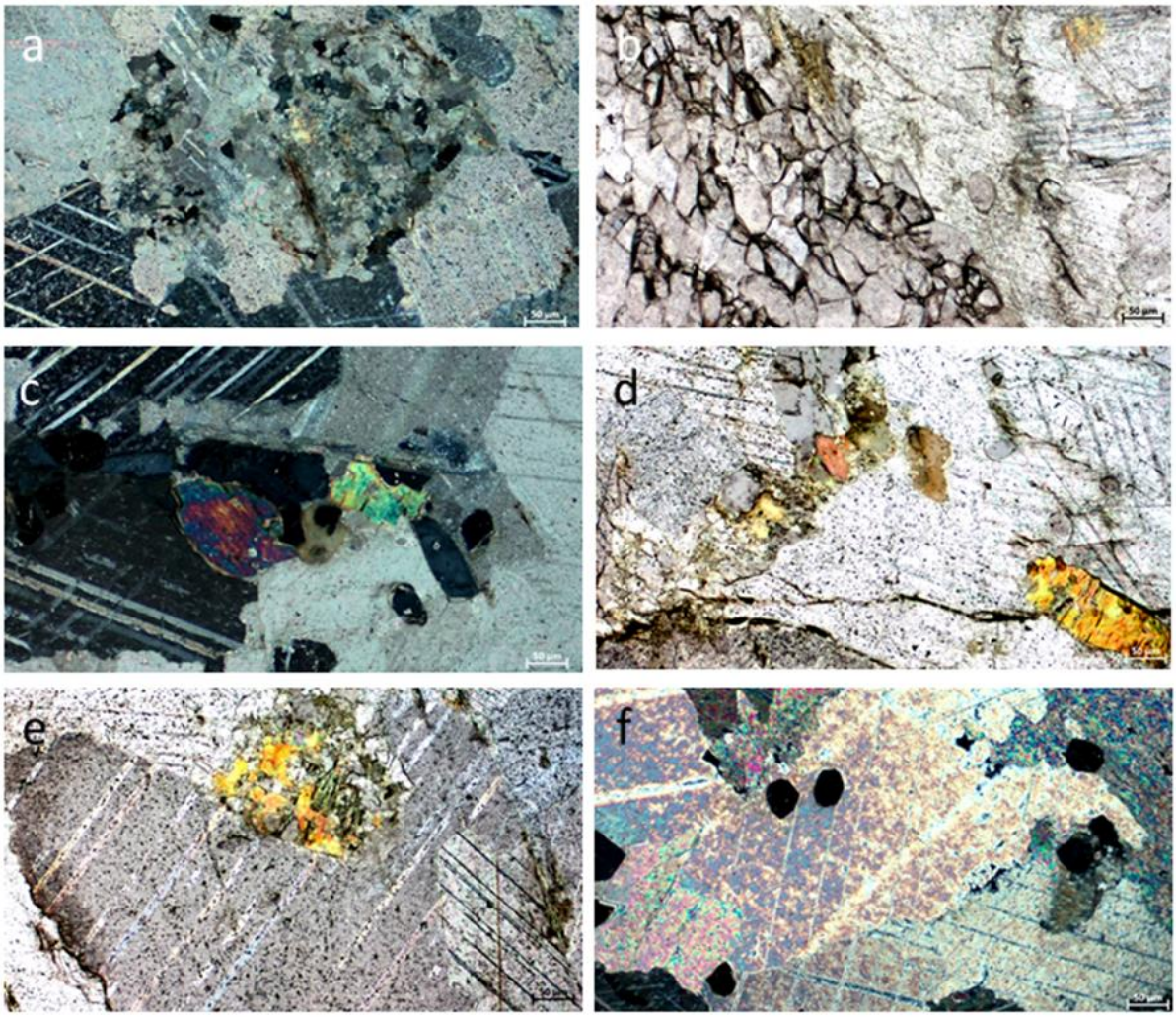

Figure 9 : Photomicrographs from sample biotite rich sovite (sample no FEN 57). (a) Coarse grained sovite showing seggreation of quartzo-feldspatic material. (b) Contact between the sovite to the right and quartzo-feldspatic material to the left. Note the higher relief, fine-grained polygonal nature of the quartzo-feldspathic material. (c) Pyroxene-biotite-apatite association in the sovite. (d) Another view of the golden brown biotites in the sovite. (e) Segregation of biotite-quartz in the close proximity of the large calcite crystals. (f) Section perpendicular to c-axis of small oval, crystals of apatite in extinction position (black). Photomicrographs a, c, f between cross nichols, all other photos in plane polarised light.

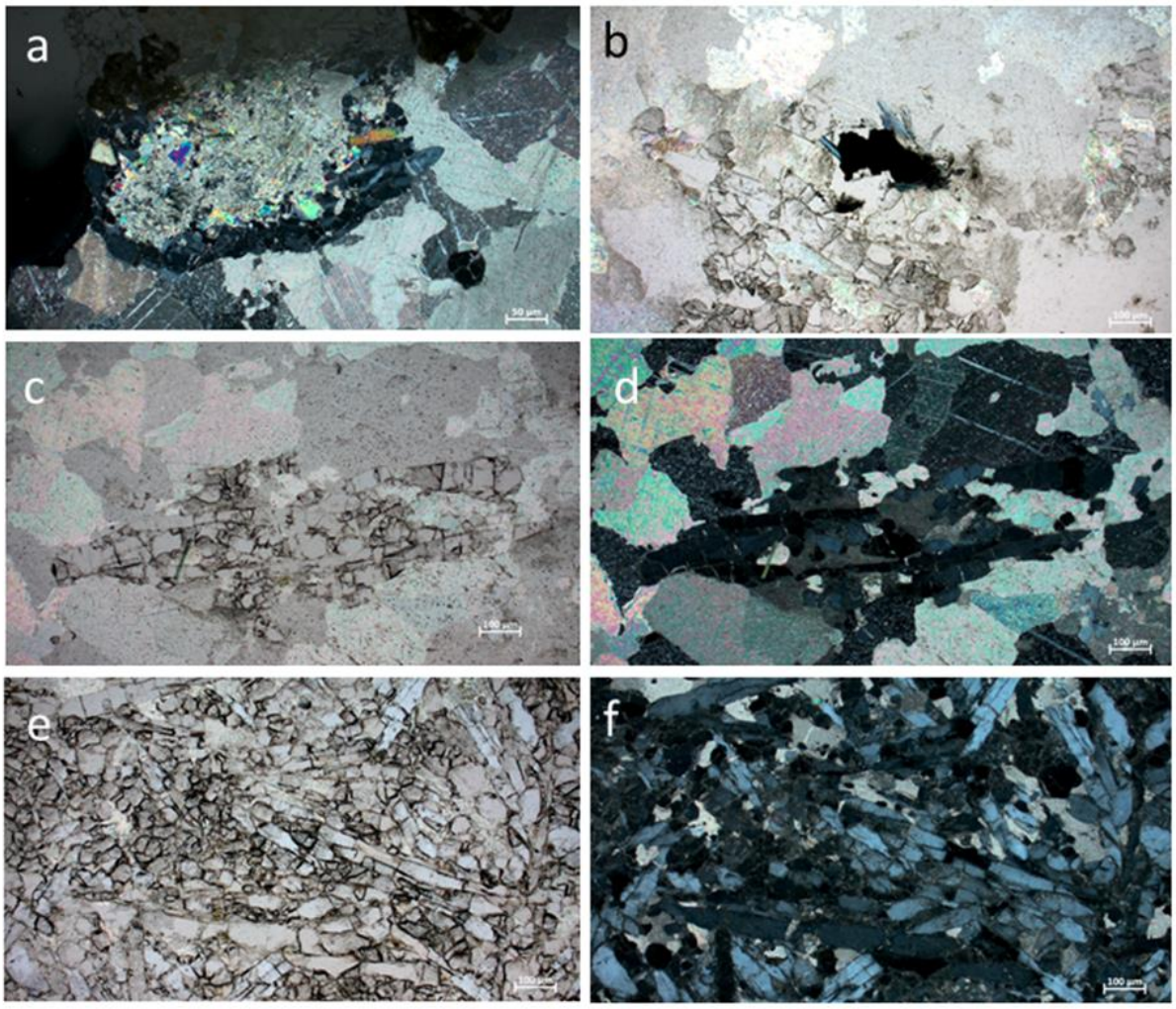

Figure 10: Photomicrographs from apatite sovite (sample FEN 73). (a) Coarse grained sovite showing coarse calcite with interlocking calcite crystals. Note the large oval segregation of quartzo-feldspatic material rimming an fine-grained aggregate of biotite-rich felsic material towards the upper edge of the tin section. (b) Slender apatite crystals adjacent to opaque (magnetite?) in an apatite-calcite groundmass. (c) Accumulation of large stout apatite crystals in the sovite carbonatite. (d) Another view of the same sovite showing strong birefringence causing the typical 'twinkling' effect when the stage of the microscope is rotated. (e) Preponderance of slender, prismatic accumulation of apatite. (f) Apatite-calcite association. Note the dull birefrence of the apatite in the section. Photomicrographs a, d, f between cross nichols, all other photos in plane polarised light.

The petrographic analysis of Fen Carbonatite complex in Norway yielded significant findings, shedding light on the mineralogical composition and textural characteristics of these rocks.
Photomicrographs revealed diverse mineral assemblages, including fenitized gneiss. (Figure 8), sovite carbonatite (Figure 9), biotite-rich soviet (Figure 10), and apatite soviet (Figure 11). Various minerals such as calcite, dolomite, bastnaesite, ankerite, biotite, feldspar, and apatite were identified, each contributing to the complex petrology of the carbonatites.

Distinct textural features were observed, including ghost crystals, pseudocubic fluorite crystals, ahedral grains of opaque minerals, and calcite phenocrysts. Additionally, the presence of sinuous veins, felsic globules, and mineral segregations highlighted the textural heterogeneity within the carbonatite samples.

The mineralogical and textural characteristics unveiled by petrographic analysis provide valuable insights into the genesis and evolution of Fen Carbonatite complex. The observed mineral assemblages and textures suggest a complex interplay of magmatic, metasomatic, and hydrothermal processes during the formation of these rocks.

3.2 XRD data

Sample Name	Minerals found	D-Spacing	Actual D	I/Io
FEN 4	Calcite	2.2914	2.495	14
		2.0918	2.095	18
		1.922	1.927	17
		1.91	1.913	17
		1.8723	1.875	18
FEN 5	Dolomite	2.8962	2.886	100
		2.1981	2.192	30
		1.7921	1.786	30
	Calcite (2-714)	2.408	2.4	30
		1.813	1.81	70
	Calcite (5-586)	2.090	2.095	18
		1.921	1.927	5
		1.870	1.875	17
	Ankerite	2.896	2.899	100
		2.198	2.199	6
		1.792	1.792	6
	Bastnaesite (11-340)??			
FEN 7	Bastnaesite	2.888	2.879	100
		2.0155	2.016	40
		1.909	1.898	40
		1.788	1.783	9
	Dolomite	2.888	2.886	100
		1.788	1.786	30
		1.5449	1.545	10
	Hematite	2.697	2.69	100
		2.516	2.51	50
		1.693	1.69	60
	Calcite (5-586)	3.0305	3.035	100
		2.281	2.285	18
		2.091	2.095	18
		1.872	1.875	17
	Hematite	2.696	2.69	100
		2.515	2.51	50
		2.206	2.201	30

FEN 6-2		1.695	1.69	60
FEN 6-3	Hematite	2.698	2.69	100
		2.515	2.51	50
		2.090	2.095	30
		1.840	1.838	40
		1.695	1.69	60
FEN 71/2	Calcite (2-714)	2.247	2.24	50
		1.847	1.85	80
	Bastnaesite	2.882	2.879	100
		2.446	2.445	9
		1.780	1.783	9
FEN 70-2	Ankerite	2.884	2.899	100
		2.428	2.411	4
		2.183	2.199	6
	Bastnaesite	2.884	2.879	100
		2.060	2.057	40
		1.780	1.783	9
	Calcite (2-714)	2.245	2.24	50
		1.847	1.85	80
	Dolomite	2.884	2.886	100
		1.801	1.804	20
		1.780	1.781	30
FEN 66/2	Magnetite	2.9627	2.967	30
		2.5225	2.532	100
		2.0879	2.099	20
		1.6153	1.616	30
	Hematite	2.693	2.69	100
		1.841	1.838	40
		1.695	1.69	60
	Bafertisite	2.5225	2.52	30
		2.229	2.23	30
		1.668	1.67	30
	Calcite (2-714)	2.962	2.95	100
		1.815	1.81	70
	Hematite	3.675	3.66	25
		2.695	2.69	100
		2.201	2.201	30

FEN 66/2A		1.839	1.838	40
		1.693	1.69	60
		2.513	2.51	50
	Calcite (5-586)	2.285	2.285	18
FEN 11	Dolomite	2.889	2.886	100
		1.777	1.786	30
	Bastnaesite	2.889	2.879	100
		1.909	1.898	40
		1.680	1.674	21
	Calcite (2-714)	2.407	2.4	30
FEN 12		2.045	2.04	40
		1.853	1.85	80
		1.555	1.56	40
	Dolomite	2.889	2.879	100
		2.195	2.192	30
		1.791	1.786	30
	Bastnaesite	2.889	2.879	100
		2.0154	2.016	40
FEN 13	Hematite	3.678	3.66	25
		2.698	2.69	100
		2.202	2.201	30
		1.838	1.838	40
		1.693	1.69	60

3.2.1 XRD Plots

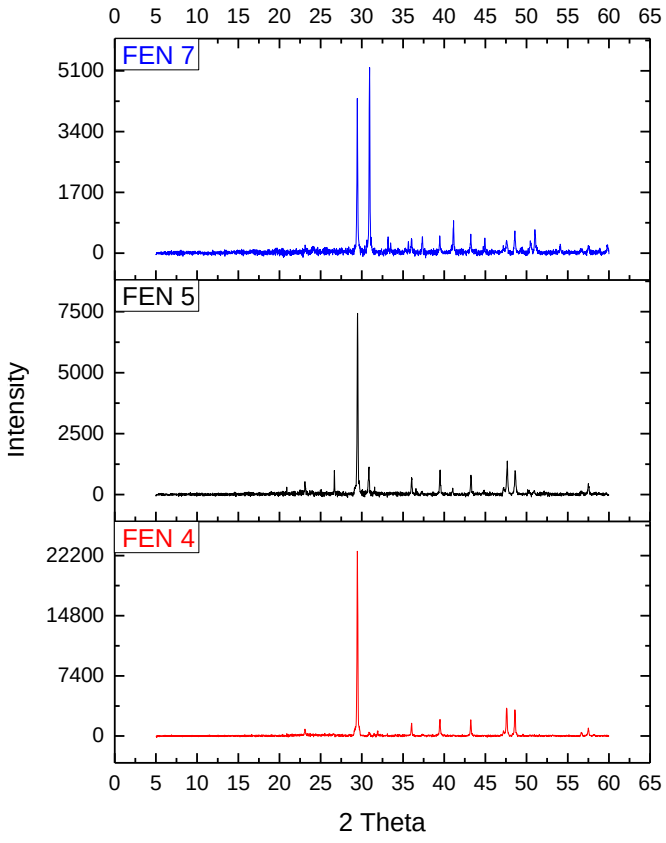

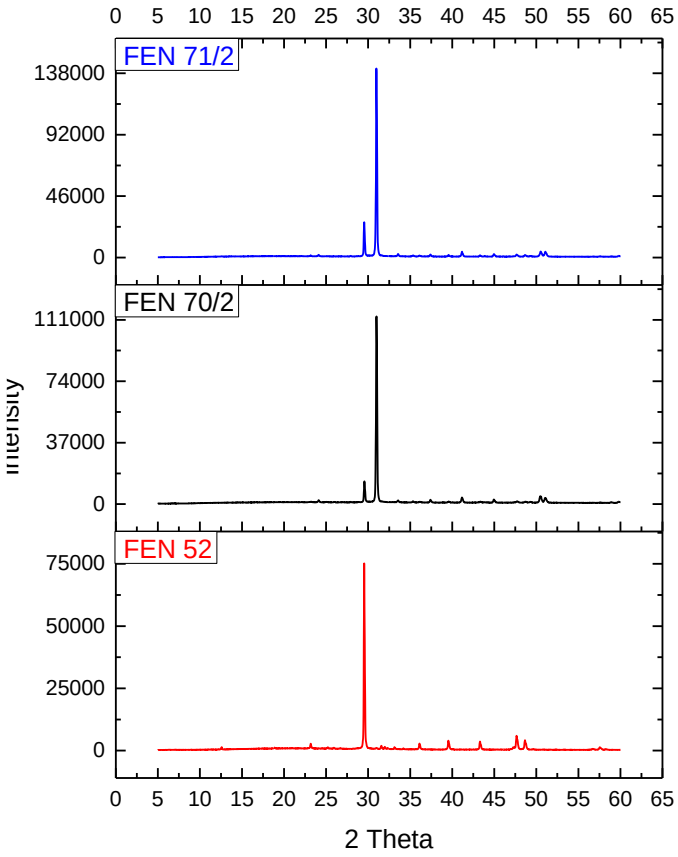

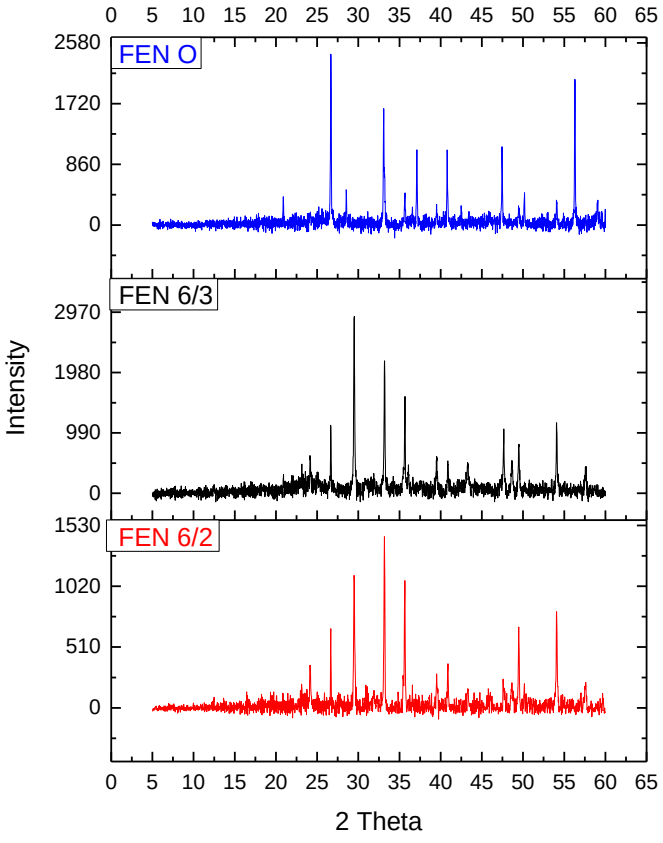

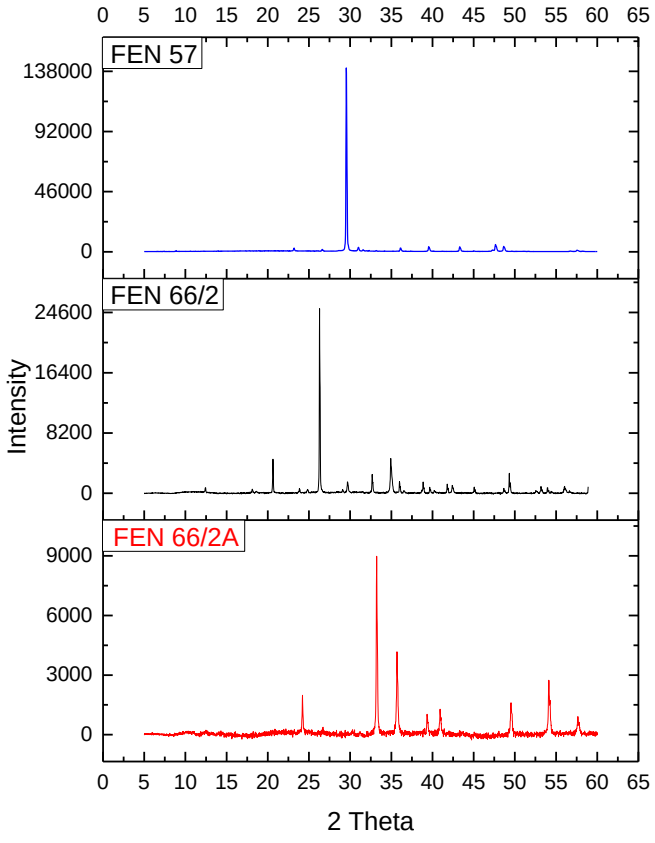

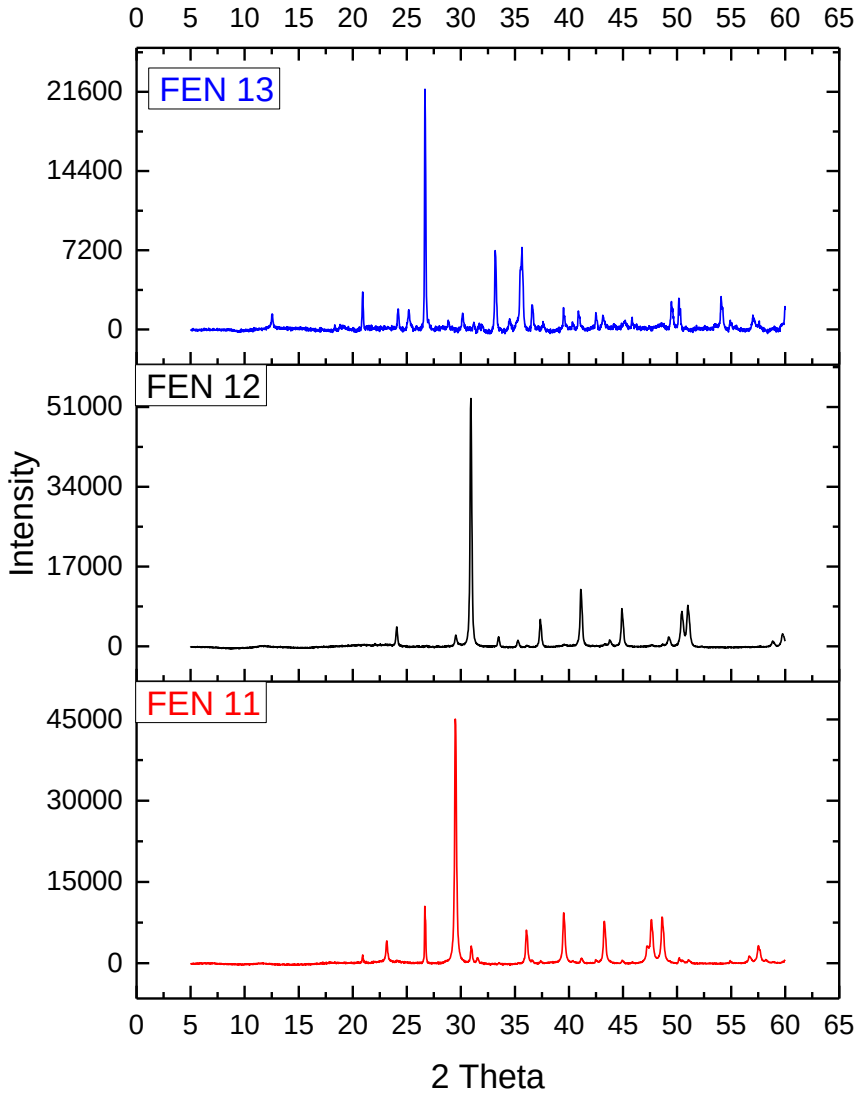

3.2.2 Discussion

The X-ray diffraction (XRD) analysis conducted on carbonatite samples from the Fen complex in Norway has yielded valuable insights into the mineralogical composition and geological significance of these rocks. Through meticulous examination of XRD data, a diverse suite of significant mineral phases including hematite, calcite, dolomite, bastnaesite, ankerite, and bafertisite, among others, were identified.

The mineralogical characteristics revealed by XRD analysis, such the presence of minerals like bastnaesite and bafertisite suggests the potential enrichment of rare earth elements (REEs), indicating magmatic or post-magmatic alteration processes.

Nevertheless, it is important to acknowledge the inherent uncertainties in XRD analysis, including limitations in mineral identification and sample heterogeneity.

Which is why I've integrated XRD data with complementary analytical techniques

(XRF, ICPMS) and geological observations, to understand the petrogenesis of Fen Carbonatite complex.

3.3 XRF data and graphs analysis

Sample	FEN4	FEN5	FEN5 Rpt	FEN7	FEN6-2	FEN6-3	KAN4	KAN5
Rock type	FOI, mnp	FOI, mnp	FOI, mnp	FOI, mnp	FOI, mnp	FOI, mnp	FOI, mnp	PB
SiO2	1.58	6.69	6.738	0.83	9.236	9.97	0.344	18.82
TiO2	0.108	0.119	0.117	0.095	0.317	0.309	0.096	0.096
Al2O3	2.935	2.755	2.73	2.397	4.093	4.553	2.352	2.741
FeOT	0.958	2.513	2.514	7.979	46.779	38.976	11.485	6.731
MnO	0.269	1.273	1.245	0.833	0.947	0.898	3.213	1.358
MgO	1.73	2.201	2.176	9.81	2.096	2.571	14.531	4.221
CaO	49.559	44.439	44.592	38.235	13.791	17.317	21	7.873
Na2O	-	-	-	-	-	-	-	-
K2O	0.186	0.024	0.024	0.024	0.072	0.077	0.024	0.024
P2O5	1.981	0.018	0.018	0.161	2.177	1.605	1.535	3.538
Total	60.093	60.228	60.346	60.58	80.311	77.356	59.725	60.811
SiO2adj	2.664	11.138	11.195	1.372	11.527	12.983	0.628	41.371
TiO2adj	0.182	0.198	0.194	0.157	0.396	0.402	0.175	0.211
Al2O3adj	4.948	4.587	4.536	3.964	5.108	5.929	4.297	6.025
Fe2O3adj	0.213	0.553	0.552	1.744	7.716	6.708	2.773	1.956
FeOadj	1.423	3.686	3.68	11.626	51.438	44.719	18.489	13.037
MnOadj	0.453	2.119	2.068	1.378	1.182	1.169	5.87	2.985
MgOadj	2.916	3.664	3.615	16.223	2.616	3.348	26.549	9.279
CaOadj	83.547	73.984	74.089	63.23	17.211	22.55	38.369	17.307
Na2Oadj	-	-	-	-	-	-	-	-
K2Oadj	0.314	0.04	0.04	0.04	0.09	0.1	0.044	0.053
P2O5adj	3.34	0.03	0.03	0.266	2.717	2.09	2.804	7.777
Or	-	-	-	-	-	-	-	0.275
An	12.494	12.382	12.243	10.684	13.608	15.779	11.196	15.071
Lc	-	-	-	-	-	-	-	-
Ne	-	-	-	-	-	-	-	-
Di	-	-	-	-	-	-	-	38.484
Hy	-	-	-	-	-	-	-	16.58
Ol	7.349	14.033	13.868	45.403	73.247	65.483	75.442	7.308
Mt	0.306	0.8	0.798	2.524	11.108	9.63	3.839	2.491
Il	0.343	0.375	0.367	0.298	0.747	0.756	0.317	0.352
Ap	7.697	0.069	0.069	0.616	6.292	4.84	6.389	18.206
Z	0.0015	0.0015	-	-	0.034	0.025	-	0.0196
Th	-	-	-	-	-	-	-	-
Cm	0.0249	0.028	0.0309	0.0266	0.041	0.0468	0.0353	0.0298
Cs	117.4336	109.618	109.8211	93.1499	16.8945	25.8388	51.7243	-
Kp	1.0472	0.1342	0.1342	0.1341	0.3001	0.3325	0.1412	-
Mg#	78.507	63.924	63.65	71.325	8.312	11.774	71.907	55.922
FeOT/MgO	0.554	1.142	1.155	0.813	22.317	15.16	0.79	1.595
Salic	12.494	12.382	12.243	10.684	13.608	15.779	11.196	15.346
Femic	7.998	15.208	15.033	48.225	85.102	75.869	79.598	45.693
CI	17.549	18.77	18.544	38.961	18.142	21.567	55.487	64.44
DI	1.0472	0.1342	0.1342	0.1341	0.3001	0.3325	0.1412	0.275
SI	59.926	46.129	45.835	54.746	4.229	6.101	55.478	38.146
AR	-	-	-	-	-	-	-	-

Sample	FEN7	FEN71/2	FEN5	FEN 4.1	FEN 52	FEN 57	FEN 70/2
Rock type	FOI, mnp	FOI, mnp	FOI, mnp	FOI, mnp	FOI, mnp	FOI, mnp	FOI, mnp
SiO2	0.934	0.532	3.768	1.6	0.869	0.686	0.248
TiO2	0.004	0.016	0.038	0.119	0.036	0.018	0.042
Al2O3	0.11	0.232	0.162	0.246	0.341	0.077	0.046
FeOT	10.421	8.3	3.722	3.198	2.291	1.317	11.195
MnO	1.151	1.9	1.775	0.381	0.449	0.385	2.254
MgO	7.061	10.008	1.476	1.37	0.827	1.012	10.205
CaO	47.006	45.851	58.576	62.079	65.634	66.517	42.564
Na2O	-	-	0.074	0.112	0.066	0.095	-
K2O	0.009	0.022	0.004	0.247	0.03	0.065	0.004
P2O5	0.139	0.069	0.007	1.478	1.767	0.679	0.064
Total	66.835	66.93	69.602	70.83	72.31	70.851	66.622
SiO2adj	1.394	0.794	5.41	2.258	1.201	0.968	0.371
TiO2adj	0.006	0.024	0.054	0.168	0.05	0.025	0.063
Al2O3adj	0.164	0.346	0.232	0.347	0.471	0.109	0.069
Fe2O3adj	2.056	1.636	0.706	0.596	0.418	0.246	2.216
FeOadj	13.71	10.908	4.708	3.976	2.79	1.637	14.772
MnOadj	1.719	2.834	2.548	0.538	0.621	0.543	3.376
MgOadj	10.543	14.928	2.119	1.933	1.143	1.428	15.284
CaOadj	70.186	68.394	84.099	87.593	90.729	93.86	63.747
Na2Oadj	-	-	0.106	0.158	0.091	0.134	-
K2Oadj	0.013	0.033	0.006	0.348	0.041	0.092	0.006
P2O5adj	0.208	0.103	0.01	2.085	2.443	0.958	0.096
An	0.409	0.847	0.14	-	0.756	-	0.17
Ne	-	-	0.486	-	0.417	0.026	-
Ac	-	-	-	1.178	-	0.712	-
Ol	38.974	44.486	13.484	9.444	6.506	5.555	50.939
Mt	2.98	2.37	1.022	0.274	0.606	-	3.211
Il	0.011	0.046	0.102	0.319	0.095	0.047	0.12
Ap	0.482	0.239	0.023	4.831	5.66	2.22	0.222
Ks	-	-	-	0.0449	-	-	-
Ns	-	-	-	-	-	0.0646	-
Cs	107.2403	104.5641	129.0922	130.3022	134.163	142.2058	97.651
Kp	0.0436	0.1108	0.0201	1.0765	0.1377	0.309	0.0201
Mg#	57.82	70.926	44.515	46.427	42.205	60.86	64.842
FeOT/MgO	1.476	0.829	2.522	2.334	2.77	1.301	1.097
Salic	0.409	0.847	0.14	-	0.756	-	0.17
Femic	41.965	46.902	14.608	10.037	7.207	5.602	54.27
CI	18.811	26.902	3.839	3.374	2.751	2.492	26.847
DI	0.0436	0.1108	0.5061	1.0765	0.5547	0.335	0.0201
SI	40.054	54.274	27.717	27.571	25.496	40.373	47.351
AR	-	-	1.003	1.012	1.003	1.005	-

3.3.1 XRF Graphs

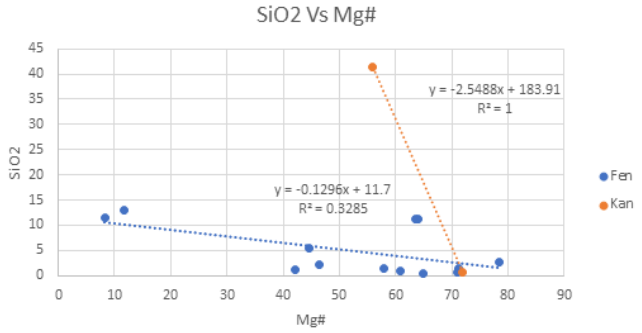

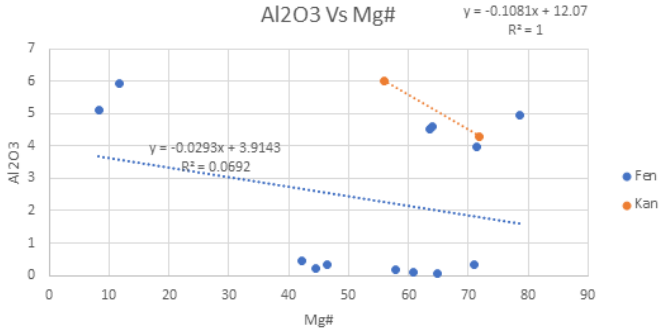

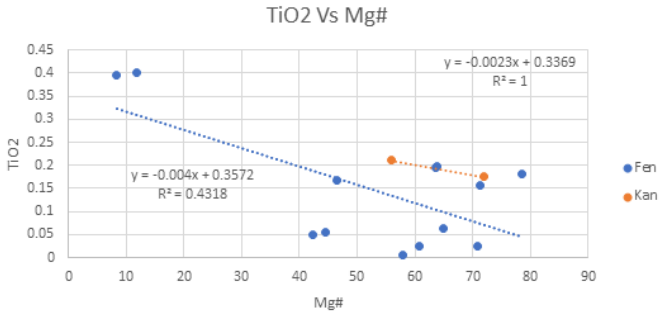

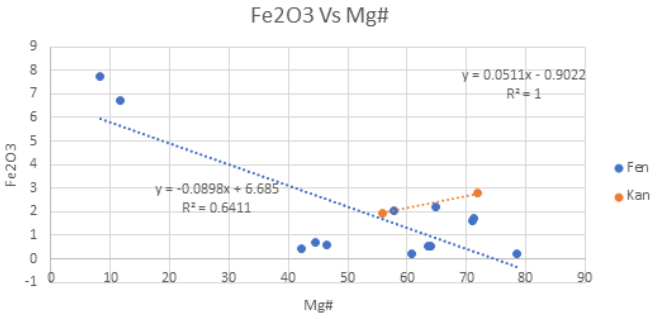

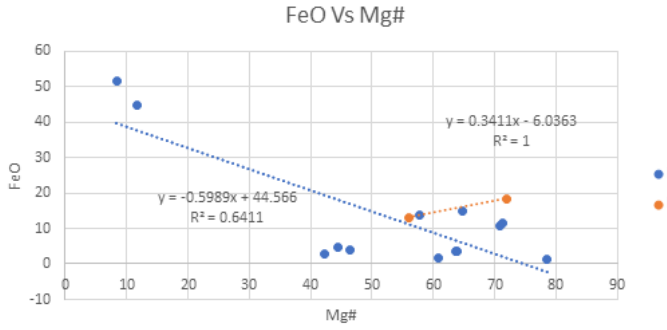

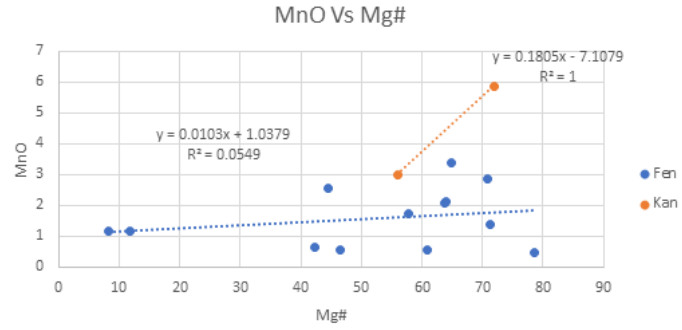

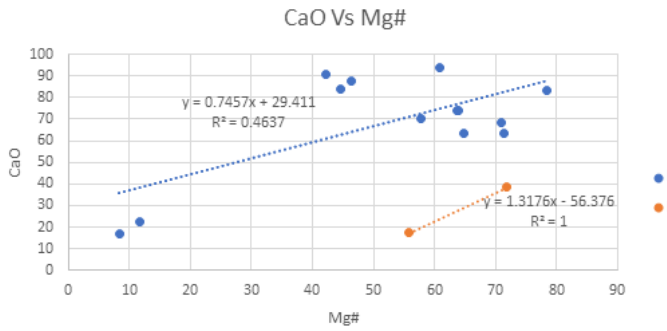

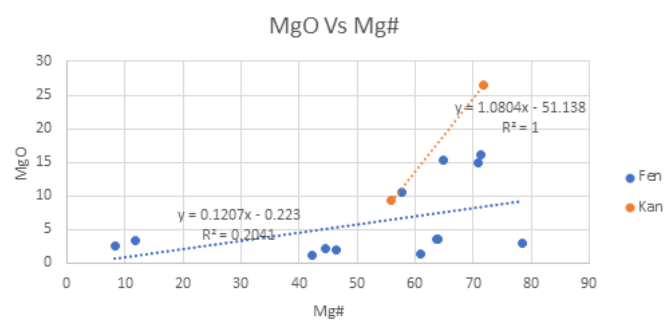

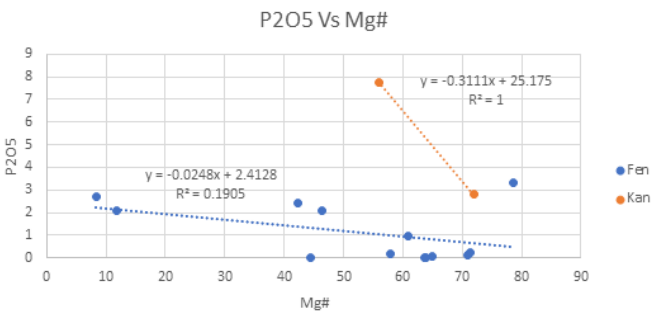

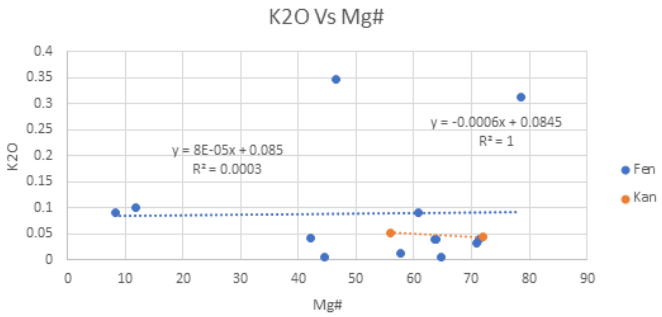

3.3.2 XRF:

The plotted trends of major oxides (SiO2, Al2O3, FeO, CaO, MgO, and P2O5) versus the Magnesium number (Mg#) for Fen and Kan carbonatite samples provide valuable insights into the petrogenesis and geochemical characteristics of these rocks.

For the Fen carbonatite samples, the SiO2-Mg# trend exhibits a negative slope (-0.1296), indicating a decrease in SiO2 content with increasing Mg# values. This suggests that the Fen carbonatites are enriched in magnesium-rich minerals and have undergone processes such as fractional crystallization or assimilation of Mg-rich mantle-derived melts.

Similarly, the Al2O3-Mg# trend also displays a negative slope (-0.0293), indicating a decrease in Al2O3 content with increasing Mg#. This may suggest a decrease in the abundance of aluminum-bearing minerals, possibly due to fractional crystallization or assimilation processes.

Conversely, the FeO-Mg# trend exhibits a positive slope (0.5989), suggesting an increase in FeO content with increasing Mg#. This could be attributed to the presence of iron-rich minerals or the influence of secondary alteration processes.

The CaO-Mg# trend shows a positive slope (0.7457), indicating an increase in CaO content with increasing Mg#. This suggests the presence of calcium-rich minerals or the influence of secondary alteration processes involving calcium.

The MgO-Mg# trend exhibits a positive slope (0.1207), reflecting an increase in MgO content with increasing Mg#. This is consistent with the notion of magnesium enrichment in carbonatite rocks.

The P2O5-Mg# trend displays a negative slope (-0.0248), indicating a decrease in P2O5 content with increasing Mg#. This may suggest a decrease in the abundance of phosphorus-bearing minerals or the influence of secondary alteration processes.

For the Kan carbonatite samples, the trends of major oxides versus Mg# exhibit similar patterns to those observed in the Fen samples but with steeper slopes and perfect correlation coefficients ($R^2 = 1$). This suggests that the geochemical characteristics of the Kan carbonatites are more homogeneous and may be indicative of a distinct petrogenetic history compared to the Fen samples.

In this study, the primary focus has been on characterizing the geochemical and petrological attributes of Fen carbonatites, with Kan serving as a comparative reference to discern any notable distinctions. The limited dataset available for Kan, comprising only two data points, was intended to provide a preliminary understanding of its geochemical signatures and ascertain its divergence from Fen carbonatites.

Overall, the observed trends in major oxides versus Mg# provide valuable insights into the petrogenesis of the carbonatite samples, suggesting processes such as fractional crystallization, assimilation, and secondary alteration have played significant roles in shaping their geochemical characteristics.

3.4 ICP-MS

	FEN4	FEN5	FEN7	FEN712	FEN702
7 Li	7.235	6.697	7.239	7.156	7.21
9 Be	0.143	0	1.004	1.291	0.43
24 Mg	19588.66	30024.02	134467.1	147814.6	139907.2
44 Ca	373640.9	377091.7	329702.4	234162.4	235867.6
45 Sc	44.629	91.583	42.494	60.774	39.711
47 Ti	263.481	89.177	136.468	267.537	89.178
51 V	17.575	10.642	117.966	27.008	17.091
52 Cr	122.694	137.656	1961.788	129.251	118.828
55 Mn	1984.551	9663.598	6242.421	7640.807	9690.837
56 Fe	8877.638	22785.08	60072.39	35914.84	49960.89
59 Co	3.11	5.151	6.512	6.706	4.762
60 Ni	32.999	50.955	49.984	50.469	53.381
63 Cu	46.217	53.053	54.175	57.236	53.767
66 Zn	103.44	123.773	165.091	104.092	230.815
71 Ga	12.254	17.7	7.318	10.212	21.785
72 Ge	1.658	1.804	1.484	1.765	2.085
75 As	3.178	2.037	2.445	5.313	1.059
78 Se	0.125	0.126	0.124	0.124	0.131
85 Rb	9.612	5.444	6.55	7.996	7.655
88 Sr	8487.843	589.693	1068.524	3602.265	4638.11
89 Y	117.323	95.078	19.835	71.331	137.064
90 Zr	117.118	158.221	124.001	670.231	6.574
93 Nb	1453.794	31.315	28.859	384.142	30.701
95 Mo	0.839	11.751	3.357	6.715	4.197
107 Ag	0.057	0.439	2.619	0.057	0.032
111 Cd	∞		∞	∞	∞
115 In	0.03	0.325	0.237	0.237	0.178
118 Sn	2.933	3.64	10.011	0.961	0.404
121 Sb	1.07	0.38	0.248	0.071	0.009
125 Te					

133 Cs	1.341	1.146	1.414	1.634	0.658
137 Ba	869.884	584.175	147.55	1927.743	10181.71
139 La	413.149	955.819	239.446	291.019	2372.218
140 Ce	653.524	2049.871	370.837	491.732	4092.877
141 Pr	85.516	334.281	43.32	65.085	575.719
146 Nd	403.373	1897.854	197.591	347.654	3060.751
147 Sm	62.932	179.622	28.189	51.788	354.671
153 Eu	20.527	52.705	10.818	19.417	111.794
157 Gd	35.029	72.614	13.866	26.637	135.017
159 Tb	7.763	7.166	2.15	5.016	19.469
163 Dy	19.991	12.388	3.379	18.02	25.622
165 Ho	4.2	3.15	1.05	3.675	4.463
166 Er	9.348	10.864	2.274	13.138	10.106
169 Tm	1.202	0.601	0.401	1.001	1.202
172 Yb	12.216	12.98	3.818	9.926	7.635
175 Lu	0.914	0.66	0.254	0.863	0.457
178 Hf	2.331	4.388	2.879	13.026	0.274
181 Ta	2.346	0.073	0	2.932	0
182 W	0.086	0.202	1.095	0.461	0.231
205 Tl	0.052	0.208	0.026	0.13	0.026
208 Pb	2.169	9.028	4.582	4.392	5.232
209 Bi	0	0.16	0.02	0.022	0.05
232 Th	26.335	289.519	13.505	112.396	461.909
238 U	11.182	11.436	2.922	6.48	8.005

3.4.1 Plots

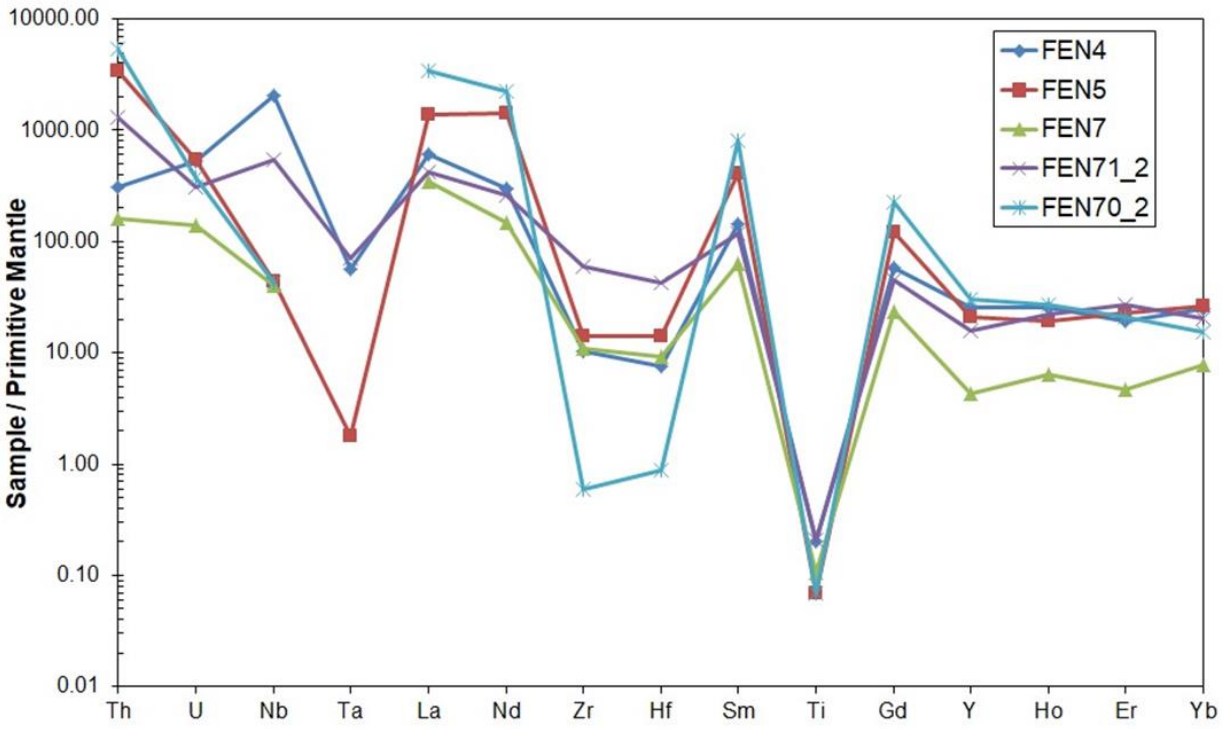

5

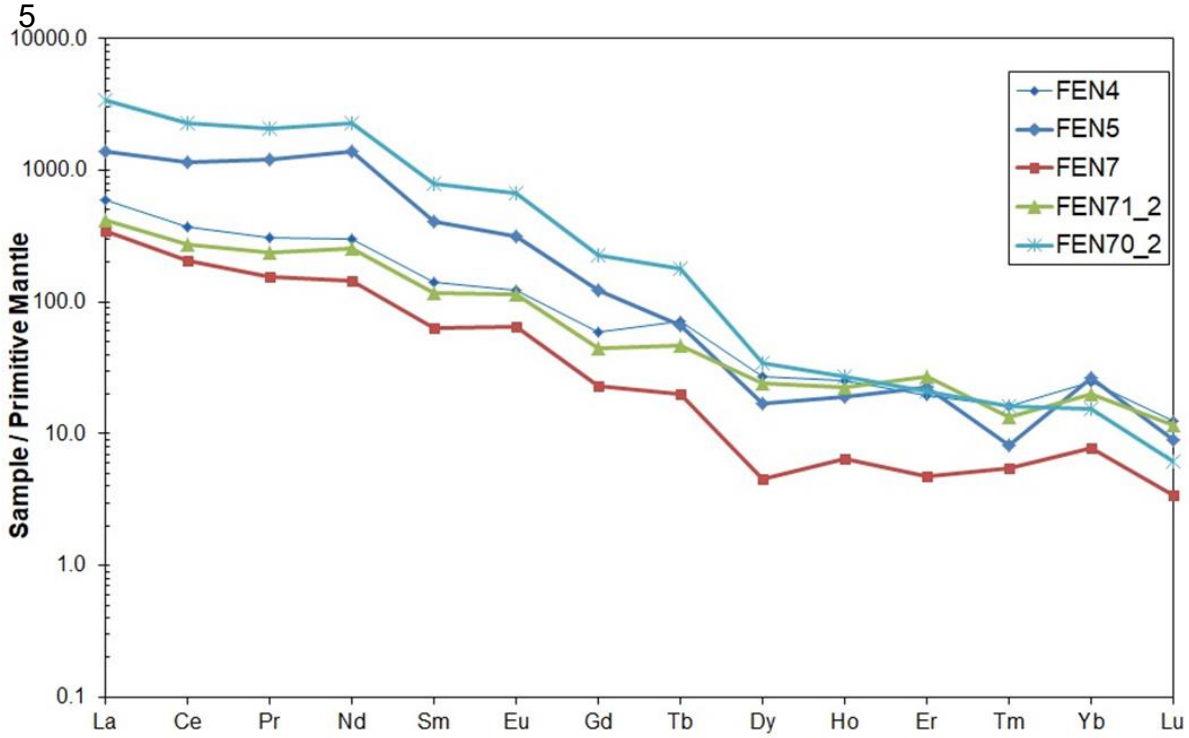

3.4.2 ICP-MS

The ICP-MS analysis conducted on the carbonatite samples has provided significant insights into their geochemical characteristics, particularly regarding rare earth element (REE) enrichments. The plotted data, with Sample/Primitive mantle on the y-axis and REE on the x-axis (from light rare earth elements, LREE, to middle rare earth elements, MREE, to heavy rare earth elements, HREE), reveals notable enrichments in REE relative to the undifferentiated mantle.

The enrichments in HREE are particularly striking, ranging from 10 to 40 times compared to the primitive mantle, indicating significant concentration anomalies. In contrast, the enrichments of MREE are even more pronounced, reaching up to 800 times in some samples, with a few displaying enrichments of up to 1000 times. Additionally, LREEs also exhibit enrichment relative to the primitive mantle.

The relative enrichment of HREEs, similar to that of the mantle, suggests a derivation from the mantle source, indicating magmatic processes. However, the exceptional enrichments observed in MREEs and LREEs, beyond what is typical for mantle-derived REE, suggest additional processes at play.

Metasomatic processes likely play a significant role in enriching the REE in these carbonatite samples. Metasomatism involves the infiltration of external fluids into the rock, altering its composition and enriching it with certain elements. The substantial enrichments observed in MREEs and LREEs could be attributed to metasomatic events, indicating interaction with external fluids rich in these elements.(Marien et al., 2018b)

Overall, the interpretation of the ICP-MS data suggests a complex petrogenetic history for the carbonatite samples. While magmatic processes contribute to the enrichment of HREEs, metasomatism plays a crucial role in enriching MREEs and LREEs. These findings underscore the dynamic nature of carbonatite formation, influenced by a combination of magmatic and metasomatic processes, and highlight the importance of considering multiple factors in understanding their petrogenesis.

Final Conclusions on the Origin of the Fen Carbonatite Complex

1. Magmatic Origin:

- REE Enrichment Patterns: The ICP-MS analysis indicates significant enrichment of REEs, especially heavy rare earth elements (HREEs), which is a typical indicator of magmatic origins. The similarity in the enrichment patterns of HREEs to the mantle suggests a mantle-derived source for the Fen carbonatites (Marien et al., 2018a)

- Petrographic Evidence: The petrographic analysis reveals primary magmatic minerals such as calcite, dolomite, apatite, and biotite, supporting a magmatic origin for the Fen carbonatites (Andersen, 1984, 1988)

- XRD Mineralogical Composition: The presence of minerals like bastnaesite and bafertisite, identified through XRD, further indicates magmatic processes as these minerals typically form during the crystallization of carbonatite magmas (Bergstøl and Svinndal, 1960).

2. Metasomatic Processes:

- Exceptional MREE and LREE Enrichments: The ICP-MS data reveal extremely high enrichments of middle rare earth elements (MREEs) and light rare earth elements (LREEs), suggesting significant modification of the original magmatic carbonatites through metasomatic processes. Interaction with external fluids, rich in these elements, likely played a crucial role (Marien et al., 2018b)

- Fluid Infiltration: Diverse mineral assemblages and textural features, such as ghost crystals and pseudocubic fluorite crystals, indicate metasomatic processes,

including fluid-rock interactions, which are capable of mobilizing and concentrating REEs (Sæther, 1957; Ramberg, 1973; Griffin and Taylor, 1975).

- Geochemical Trends: The plotted trends of major oxides versus Mg# suggest that fractional crystallization and metasomatic alteration have influenced the Fen carbonatites. Negative slopes for SiO_2, Al_2O_3, and P_2O_5 with Mg# indicate depletion during metasomatic alteration, while positive slopes for FeO, CaO, and MgO suggest enrichment through these processes (Meert et al., 1998).

3. Hydrothermal Influences:

- Fluid Evolution: The presence of melt and fluid phases in carbonatite systems to lower temperatures, along with the evolution of carbonatite melts by fractionating minerals like calcite, apatite, and dolomite, points to significant hydrothermal activity. These processes can concentrate incompatible elements such as alkalis, halides, and sulfate, contributing to the geochemical complexity of the Fen carbonatites (Brogger, 1921; Andersen, 1984, 1988).

- Para magmatic and Post magmatic Fluids: Distinguishing between syn magmatic, para magmatic, and post magmatic fluids highlight the dynamic fluid evolution within the Fen carbonatite system. These fluids can cause auto metasomatism and substantial overprinting of the original mineral assemblages (Marien et al., 2018a).

Summary

The Fen Carbonatite Complex exhibits a complex petrogenetic history influenced by a combination of magmatic, metasomatic, and hydrothermal processes. The primary magmatic origin is evident from the REE enrichment patterns and petrographic analysis. However, metasomatic and hydrothermal processes have significantly modified the original magmatic carbonatites, enriching them in MREEs and LREEs, and altering their mineralogical and geochemical characteristics. The integration of multiple analytical techniques—ICP-MS, petrography, XRD, and XRF—has been crucial in unraveling the intricate history of the Fen Carbonatite Complex, underscoring the necessity of a multi-faceted approach in geological research (Mitchell & Brunfelt, n.d.).

Bibliography

Andersen, T. (1984). Secondary processes in carbonatites: petrology of “rodberg” (hematite-calcite-dolomite carbonatite) in the Fen central complex, Telemark (South Norway). In *Lithos* (Vol. 17).

Andersen, T. (1988). Evolution of peralkaline calcite carbonatite magma in the Fen complex, southeast Norway. In *Lithos* (Vol. 22).

Marien, C., Dijkstra, A. H., & Wilkins, C. (2018a). The hydrothermal alteration of carbonatite in the Fen Complex, Norway: mineralogy, geochemistry, and implications for rare-earth element resource formation. *Mineralogical Magazine*, *82*(S1), S115–S131. https://doi.org/10.1180/minmag.2017.081.070

Marien, C., Dijkstra, A. H., & Wilkins, C. (2018b). The hydrothermal alteration of carbonatite in the Fen Complex, Norway: mineralogy, geochemistry, and implications for rare-earth element resource formation. *Mineralogical Magazine*, *82*(S1), S115–S131. https://doi.org/10.1180/minmag.2017.081.070

Mitchell, R. H., & Brunfelt, A. O. (n.d.). *Rare Earth Element Geochemistry of the Fen Alkaline Complex, Norway*.

Ramberg, I. B. (n.d.). *Gravity Studies of the Fen Complex, Norway, and Their Petrological Significance**.

Streckeisen, A. (1979). *Classification and nomenclature of volcanic rocks, lamprophyres, carbonatites, and melilitic rocks: Recommendations and suggestions of the IUGS Subcommission on the Systematics of Igneous Rocks*. http://pubs.geoscienceworld.org/gsa/geology/article-pdf/7/7/331/3551711/i0091-7613-7-7-331.pdf

Verma, S. P., Torres-Alvarado, I. S., & Sotelo-Rodr, Z. T. (2002). SINCLAS: standard igneous norm and volcanic rock classification system $. In *Computers & Geosciences* (Vol. 28). http://www.iaing.org/

Yaxley, G. M., Anenburg, M., Tappe, S., Decree, S., & Guzmics, T. (2022). *Carbonatites: Classification, Sources, Evolution, and Emplacement*. https://doi.org/10.1146/annurev-earth-032320

Bergstøl, S., & Svinndal, S. (1960). Geological Features of Fen Complex

Brogger, W. C. (1921). Location and Significance of Fen Complex

Griffin, W. L., & Taylor, P. N. (1975). Petrographic Analysis

Meert, J. G., et al. (1998). Dating of Ultramafic Lamprophyres

Sæther, E. (1957). Petrogenetic Studies on Fen Complex